Decay analysis of light mass compound nucleus ^{70}As* formed in ^{6}Li induced reaction

Gayatri Sarkar[1,2*] and Manoj K. Sharma[3]
[1] *Department of Physics, Indian Institute of Technology Roorkee, Roorkee 247667, India*
[2] *Noida Institute of Engineering and Technology, Knowledge Park-II, Institutional Area, Greater Noida (UP) - 201306, INDIA and*
[3] *School of Physics and Materials Science, Thapar Institute of Engineering and Technology, Patiala-147004, INDIA*

Introduction

In general, all possible target-projectile combinations produce an excited compound nucleus (CN) that disintegrates into binary fragments at various extremities, including excitation energy/temperature, angular momentum, deformations, orientations, etc. The de-excitation of the CN, based on these parameters, may result in a variety of decay mechanisms, including evaporation residues (ERs), intermediate-mass fragments (IMFs), heavy-mass fragments (HMFs), and fission fragments (FFs). The dominance of these decay modes varies according to CN's mass and excitation energy. This work will concentrate on the ERs, the sole contributor to the fusion process.

Methodology

Dynamical Cluster-decay Model (DCM) [1] which is based on the collective clusterization approach of Quantum Mechanical Fragmentation Theory [2], and works in terms of the collective coordinates such as mass asymmetry parameter (η_A), relative separation R between two fragments, multipole deformations $\beta_{\lambda i}$ and orientations θ_i (where, $i = 1, 2$ for heavy and light fragment) is applied to study the decay dynamics of CN. The deformation parameters are also made temperature dependent, by using the relation: $\beta_{\lambda i}(T) = exp(-T/T_0)\beta_{\lambda i}(0)$, where $\beta_{\lambda i}(0)$ represents the static deformation and T_0 is the temperature of the nucleus at which shell effects start to vanish (T_0 = 1.5 MeV). Using these coordinates, the fragmentation potential $V(\eta, T)$ is calculated at a fixed R as, $V(\eta, T) = -\sum_{i=1}^{2}[B_i(A_i, Z_i, T)] + V_C + V_P + V_\ell$. B_i, V_C, V_P, and V_ℓ are, respectively, the binding energy, Coulomb interaction, nuclear proximity, and centrifugal potentials [1]. $V(\eta, T)$ is further used as an input in Schrödinger equation of η-coordinate to obtain preformation probability P_0 of decaying fragments as: $P_0 = |\psi[\eta(A_i)]|^2 \frac{2}{A_{CN}}\sqrt{B_{\eta\eta}}$. $B_{\eta\eta}$ are the smooth hydrodynamical mass parameters. The CN decay cross-section is calculated using the ℓ partial waves method. For more details see [3].

Results and discussion

The CN is studied using a reformulated DCM to examine the role of one of the main ingredients of the model, namely, the temperature-dependent binding energy, *i.e.*, Krappe Binding Energy [4]. With the proper inclusion of temperature-dependent Wigner and pairing energies, the fully T-dependent reformulated DCM is applied to study the ^{6}Li+^{64}Zn reaction [5]. Our theoretical work analyzed the decay mechanism of light-mass Arsenic isotope, *i.e.*, ^{70}As*, produced through the above-considered reaction at $E_{c.m.}$= 21.94 MeV. To build on the above idea, the mass fragmentation of ^{70}As* is investigated using spherical, static [β_2 (T=0)], and dynamic [β_2 ($T \neq$0)] quadrupole deformations with optimum orientations ($\theta_i^{opt.}$) within the DCM as given in Fig. 1. The decay fragments are $1n$, ^{2}H, ^{3}H, and ^{4}He, irrespective of the choice of deformation parameter. The correspond-

*Electronic address: gayatri11.sarkar@gmail.com

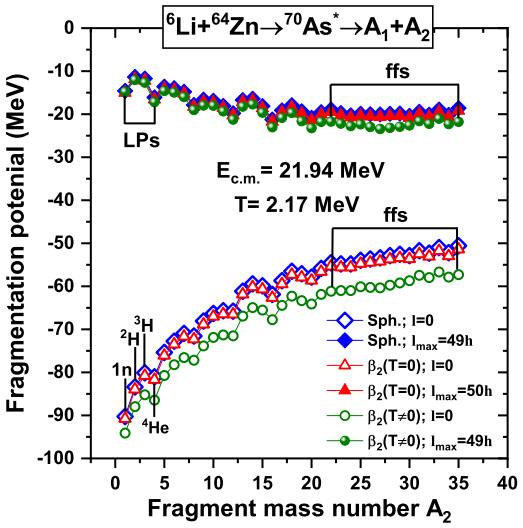

FIG. 1: The fragmentation potential $V_R(\eta, T)$ as a function of fragment mass number A_2 for the decay of ^{70}As* CN at $E_{c.m.}$=21.94 MeV.

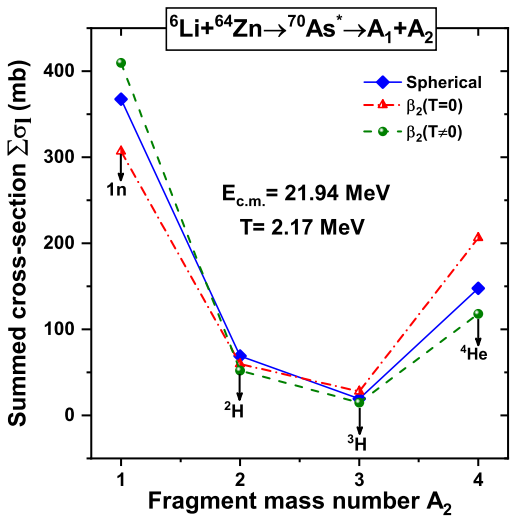

FIG. 2: The variation of the total cross-section with respect to fragment mass number A_2 for the decay of ^{70}As* CN at $E_{c.m.}$=21.94 MeV.

ing second-order deformations are negative for heavier decay fragments (A_1), and they are oblate-shaped. In contrast, lighter decay fragments (A_2) are spherical. At ℓ=0 angular momentum, the fragmentation structure indicates that spherical and static β_2 deformations coincide in ERs and fission regions. Incorporating the dynamic β_2 deformations, there is a difference in the structure, particularly in the fission region. The fragmentation structures at maximum angular momentum overlap for spherical, static, and dynamic β_2 deformations. Moreover, in the total cross sections, the penetrability of the decay fragments plays a significant role. Due to the lower barrier height, the penetrability of $1n$ decay across the potential barrier is larger for spherical configuration than in static or dynamic β_2 configurations. The penetrability of other contributing fragments is similar to that of $1n$, irrespective of the choice of deformation. However, all three configurations can reproduce the experimental cross-sections at the considered energy with its optimized neck-length parameter (ΔR) as given in Table I.

TABLE I: The total fusion cross-section (σ_{fus}=σ_{ER}) for the CN ^{70}As* have been estimated using DCM and compared with the experimental cross-sections [5] at T=2.17 MeV.

$E_{c.m.}$	Spherical		β_2-(T=0)		β_2-(T≠0)		
	ΔR	σ	ΔR	σ	ΔR	σ	$\sigma_{expt.}$
(MeV)	(fm)	(mb)	(fm)	(mb)	(fm)	(mb)	(mb)
21.94	0.62	603.4	0.26	600.2	0.57	594.7	597±45

Acknowledgement

The fellowship from the Ministry of Human Resource & Development, Government of India, is gratefully acknowledged by G.S.

References

[1] R. K. Gupta *et al.*, Phys. Rev. C **71** 014601 (2005).

[2] J. Maruhn *et al.*, Phys. Rev. Lett. **32** 548 (1974).

[3] R. K. Gupta *et. al*, Phys. Rev. C **70**, 034608 (2004).

[4] H. J. Krappe *et al.*, Phys. Rev. C **59** 2640 (1999).

[5] I. Padron *et al.*, Phys. Rev. C **66** 044608 (2002).